

RECENT THEORETICAL RESULTS ON CORONAL HEATING

DANIEL O. GOMEZ^{1,*}, PABLO A. DMITRUK^{1,†} and LEONARDO J. MILANO^{2,†}

¹*Department of Physics, University of Buenos Aires, Ciudad Universitaria,
1428 Buenos Aires, Argentina*

²*National Solar Observatory, P.O.Box 62, Sunspot, NM 88349, U.S.A.*

(Received 20 September 1999; accepted 1 March 2000)

Abstract. The scenario of magnetohydrodynamic turbulence in connection with coronal active regions has been actively investigated in recent years. According to this viewpoint, a turbulent regime is driven by footpoint motions and the incoming energy is efficiently transferred to small scales due to a direct energy cascade. The development of fine scales to enhance the dissipation of either waves or DC currents is therefore a natural outcome of turbulent models. Numerical integrations of the reduced magnetohydrodynamic equations are performed to simulate the dynamics of coronal loops driven at their bases by footpoint motions. These simulations show that a stationary turbulent regime is reached after a few photospheric times, displaying a broadband power spectrum and a dissipation rate consistent with the energy loss rates of the plasma confined in these loops. Also, the functional dependence of the stationary heating rate with the physical parameters of the problem is obtained, which might be useful for an observational test of this theoretical framework.

1. Introduction

Recent X-ray and EUV observations of the solar corona reveal a highly structured brightness distribution, which is the consequence of magnetic fields confining the X-ray emitting plasma and governing its dynamics. Observations made with high spatial resolution (Schrijver *et al.*, 1999; Golub *et al.*, 1990; Golub and Pasachoff, 1997) show coronal magnetic loops with a highly filamentary internal structure.

Coronal heating theories have traditionally been classified into two broad categories: (a) *AC or wave models*, for which energy is provided by waves generated at the photosphere and, (b) *DC or stress models*, which assume that energy dissipates in magnetic stresses driven by slow footpoint motions. Although these two concepts seem mutually exclusive, the following assumptions are shared by both classes of models: (i) the ultimate source for coronal heating is the kinetic energy of the photospheric velocity field, (ii) the dissipation mechanism is Joule heating, although viscosity might also play an important role, (iii) the existence of fine structure in the coronal magnetic field is invoked to speed up Joule (or viscous) dissipation. Recent review articles on coronal heating (Narain and Ulmschneider,

*Also at: Instituto de Astronomía y Física del Espacio, C.C.67, Suc.28, 1428 Buenos Aires, Argentina.

†Presently at: Bartol Research Institute, University of Delaware, Newark, DE 19716, U.S.A.



1996, 1990; Gómez, 1990; Zirker, 1993), explore the various theoretical models in further detail.

As mentioned, the natural candidate for the energy dissipation is Joule heating, but the typical time scale to dissipate coronal magnetic stresses on the length scale of the driving photospheric motions is exceedingly long. This time-scale can be estimated as $l^2/\eta \sim 10^6$ years ($l = 10^3$ km: length scale of photospheric motions, $\eta = 10^3$ cm² s⁻¹: resistivity). Therefore, most of the current theories of coronal heating deal with different mechanisms to speed up dissipation (Parker, 1972, 1983; Heyvaerts and Priest, 1983; van Ballegoijen, 1986). Numerical integrations of the MHD equations have also been performed (Mikic, Schnack, and van Hoven, 1989; Longcope and Sudan, 1994), to study the dynamics of coronal loops driven at their bases by convective motions. These simulations show the development of small spatial structures (current sheets), which contribute to enhance dissipation.

One of the promising scenarios is the assumption that the magnetic and velocity fields of the coronal plasma are in a turbulent state (Gómez and Ferro Fontan, 1988, 1992; Heyvaerts and Priest, 1992; Einaudi *et al.*, 1996; Hendrix and van Hoven, 1996; Dmitruk and Gómez, 1997). Since the dynamics of coronal loops is dominated by their magnetic field, turbulent fluctuations of both the velocity and the magnetic fields are generated predominantly in the directions perpendicular to the main magnetic field (for details on the MHD turbulent scenario, see, for instance Biskamp, 1993). In a turbulent regime, energy is transferred from photospheric motions to the magnetic field. This energy cascades toward small scales due to nonlinear interactions, until highly structured electric currents are formed. The development of fine scales to enhance the dissipation of either waves or DC currents, is therefore a natural outcome of turbulent models. On the other hand, the dynamics of the solar photosphere is dominated by its velocity field, and therefore an essentially hydrodynamic turbulence is observed in this region (Nesis *et al.*, 1999).

We present numerical integrations of the reduced magnetohydrodynamic equations, to simulate the dynamics of coronal loops driven at their bases by footpoint motions. These simulations show that after a few photospheric turnover times a stationary turbulent regime is reached, displaying a broadband power spectrum and a dissipation rate consistent with the energy loss rates of the plasma confined in these loops. In Section 2 we briefly describe recent observational results which are relevant to the problem of coronal heating. The reduced MHD approximation is described in Section 3, and various results from recent numerical simulations of the RMHD equations are summarized in Section 4. An interesting scaling law, which relates the heating rate with the physical parameters of the loop is given in Section 5. A statistics of dissipation events arising from time-extended 2D MHD simulations, which displays a slope quite comparable to those reported for flare (Hudson, 1991) and microflare (Shimizu, 1995) events, is shown in Section 6. Finally, in Section 7 we summarize our conclusions.

2. Recent Observational Results

The Transition Region and Coronal Explorer (TRACE) is showing us the spatial structure and dynamics of the solar corona with unprecedented quality. Active regions observed by TRACE are composed by bundles of long and thin loops displaying a highly dynamic behavior, which involve not only kinematic motions of the magnetic structure, but also rapid changes in the temperature and density of individual loops.

The extremely dynamic nature of coronal loops is suggestive of a rather intermittent heating process, both in space and time. Typical time-scales for this variability are a few minutes or less, while spatial structures of all sizes are observed, down to the resolution limit of 700 km (Schrijver *et al.*, 1999). A spatially intermittent heating would qualitatively explain the rich transverse structure, since only those field lines connected to locations where heating pulses occur will light up. On the other hand, a temporally intermittent heating would force these loops to adjust their internal structures, i.e., their densities, temperatures and longitudinal velocities. In some active regions, transverse oscillations of loops have also been observed, and it has been suggested that the kinetic energy associated to these oscillations might play a role in the heating of the region (Nakariakov *et al.*, 1999).

3. Reduced MHD Approximation

In view of the observed features mentioned above, in what follows we concentrate on the theoretical description of a relatively homogeneous bundle of field lines. The loop footpoints are deeply rooted into the photosphere, which moves individual field lines around, thus generating magnetic stresses in the coronal portion of the loop. Two important time-scales arise in this process: the Alfvén time, t_A , which is the time it takes for an Alfvén wave to travel along the loop; and the photospheric time t_p , which is the turnover time of photospheric granules. If $t_A \gg t_p$, i.e., if the driving time-scale is much shorter than the response time of the loop, AC heating processes might be important (Ionson, 1982; Heyvaerts and Priest, 1983; Hollweg, 1985; Ofman, Davila, and Steinolfson, 1995). On the other hand, whenever $t_A \ll t_p$, DC heating is dominant. Under the assumption that a coronal loop reaches a stationary turbulent state, its response to a broad range of photospheric driving frequencies can be modeled by a closure model. At least for photospheric power spectra decreasing as power laws of both the wavenumber and the time frequency, the heating of the loop is dominated by DC heating (Milano, Dmitruk, and Mandrini, 1997) (see also Heyvaerts and Priest (1992) and Gómez and Ferro Fontán (1992) for closure models applied to a magnetic arcade and to a loop driven by stationary footpoint motions, respectively).

In the present paper, the aim is to study the heating of a topologically simple loop, which can be regarded as a sub-structure or building block of the much more

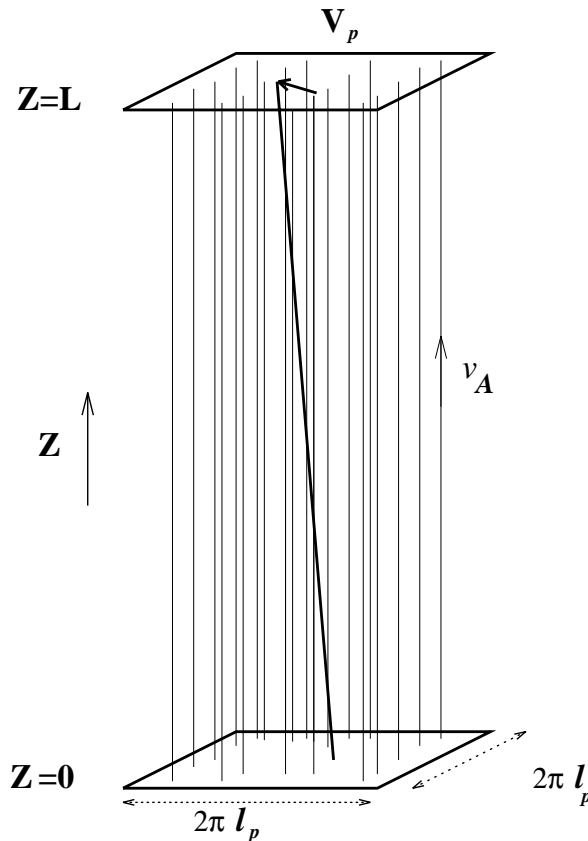


Figure 1. Perturbed field line in a coronal loop. The planes $z = 0$ and $z = L$ represent the photosphere.

complex active regions. The idea behind this approach is that if we manage to explain the heating of simple loops, then we should be able to explain the heating of complex superpositions of these structures, although it seems clear that complex structures might provide extra heating. Furthermore, we take advantage of the (typically) large aspect ratio of observed loops and *straighten them up*, thus neglecting toroidal effects, i.e., effects arising from the curvature of loops. Also, oscillatory motions of the loop as a whole are neglected, as well as its interactions with other magnetic structures.

We therefore consider a simplified model of a coronal magnetic loop with length L and cross section $2\pi l_p \times 2\pi l_p$, where l_p is the length scale of typical photospheric motions. For elongated loops, i.e., such that $2\pi l_p \ll L$, it is reasonable to neglect toroidal effects. The main magnetic field \mathbf{B}_0 is assumed to be uniform and parallel to the axis of the loop (the z axis). The planes at $z = 0$ and $z = L$ correspond to the loop footpoints at the photosphere, as shown in Figure 1.

Under these assumptions, we are able to use the reduced MHD approximation (Strauss, 1976), in which the plasma moves incompressibly in planes perpendicular to the axial field \mathbf{B}_0 , and the transverse component of the magnetic field is small compared to \mathbf{B}_0 . The very high electric conductivity (frozen field) allows photospheric motions to easily drive magnetic stresses in the corona (Parker, 1972), the field lines twist and bend due to these motions and this generates transverse components of velocity \mathbf{u} and magnetic field \mathbf{b} . Therefore:

$$\mathbf{B} = B_0\mathbf{z} + \mathbf{b}(x, y, z, t), \quad \mathbf{b} \cdot \mathbf{z} = 0, \quad (1)$$

$$\mathbf{u} = \mathbf{u}(x, y, z, t), \quad \mathbf{u} \cdot \mathbf{z} = 0. \quad (2)$$

Since both \mathbf{b} and \mathbf{u} are two-dimensional and divergence-free fields, they can be represented by scalar potentials:

$$\mathbf{b} = \nabla \times (a\mathbf{z}) = \nabla a(x, y, z, t) \times \mathbf{z}, \quad (3)$$

$$\mathbf{u} = \nabla \times (\psi\mathbf{z}) = \nabla \psi(x, y, z, t) \times \mathbf{z}, \quad (4)$$

where ∇ indicates derivatives in the x, y plane.

The reduced MHD equations for the potentials ψ and a are (Strauss, 1976):

$$\partial_t a = v_A \partial_z \psi + [\psi, a] + \eta \nabla^2 a, \quad (5)$$

$$\partial_t w = v_A \partial_z j + [\psi, w] - [a, j] + \nu \nabla^2 w, \quad (6)$$

where vorticity w and current density j relate to the potentials as

$$w = -\nabla^2 \psi, \quad j = -\nabla^2 a. \quad (7)$$

The brackets $[A, B] = \partial_x A \partial_y B - \partial_y A \partial_x B$ are the standard Poisson brackets and $v_A = B_0 / \sqrt{4\pi\rho}$ is the Alfvén velocity (ρ is the plasma density).

Equation (5) describes the advection of the potential a and Equation (6) corresponds to the evolution of vorticity w . The terms $v_A \partial_z$ represent the coupling between neighboring $z = \text{constant}$ planes. The role of these terms is to transfer energy from the footpoints into the coronal part of the loop. The ∇^2 terms represent dissipative effects, the constants η and ν being the resistivity and viscosity coefficients. The nonlinear terms are those represented by the Poisson brackets. Their role is to couple normal modes in such a way that energy, and other ideal invariants, can be transferred between them. The fields \mathbf{u} and \mathbf{b} depend on the axial z -coordinate, although their nonlinear interaction proceeds independently on different constant z planes across the loop.

4. Turbulent Heating

Since the Reynolds numbers in coronal active regions are extremely large ($R \sim S \sim 10^{10-12}$) we can expect coronal loops to be in a strongly turbulent regime. Although the theoretical framework for the study of turbulence was first developed for non-magnetic fluids, thanks to the pioneering work of Kolmogorov, the following general description applies to either hydrodynamic or magnetohydrodynamic turbulent regimes. The effect of nonlinear terms is to redistribute excitations from one wavenumber to another in a rather stochastic fashion. Only those excitations at sufficiently large wavenumbers decay as a consequence of dissipative effects. Therefore, a net flow of excitations in Fourier space is established, toward those regions which are deficient with respect to the values calculated from an ideal (without dissipation) model (Montgomery, 1983). As a result, this nonlinear redistribution continuously replenishes the excitations being drained at the large wavenumber region. An increase in Reynolds number only raises the value of the typical wavenumber at which dissipation begins to dominate, but does not inhibit the excitation flow in Fourier space. According to this scenario, three regions in Fourier space (wavenumbers space) can be identified, each of them displaying a different turbulent behavior, as sketched in Figure 2:

(1) *The energy-containing region*: Comprises those modes that are being excited directly by the external driver, which is usually located at low wavenumbers. However, it does not necessarily include the very lowest wavenumbers, which are determined by the size of the system.

(2) *Dissipation region*: Corresponds to those modes where fluctuations are being efficiently quenched by dissipative (viscous or ohmic) effects. This region is normally located at the largest wavenumbers, where the linear dissipative terms become comparable to the nonlinear terms.

(3) *Energy inertial region*: In this region, external forces and dissipation are both negligible. Only nonlinearities play a role, transferring fluctuations from one mode to another, while keeping the total energy constant. This region normally bridges the gap between the low wavenumber energy containing region and the large wavenumber dissipative zone.

Kolmogorov (1941), following heuristic arguments, has shown that when a three dimensional incompressible fluid is submitted to external forcing with a narrow spectrum, a direct energy cascade is generated and a stationary energy spectrum is achieved, displaying the well known $k^{-5/3}$ distribution in the energy inertial region (see Figure 2). Kolmogorov's ideas, mainly based on scaling properties of the ideal equations and on the existence of a net energy flow through the corresponding inertial range, are usually known as *cascade theory* and have been applied to a number of turbulent systems including two and three-dimensional MHD turbulence (Montgomery, 1983). The power spectra predicted by cascade theory for the energy inertial range, have in many cases been confirmed by experiments (Grant, Stewart, and Molliet, 1962; Matthaeus and Goldstein, 1982; Sommeria, 1986) and

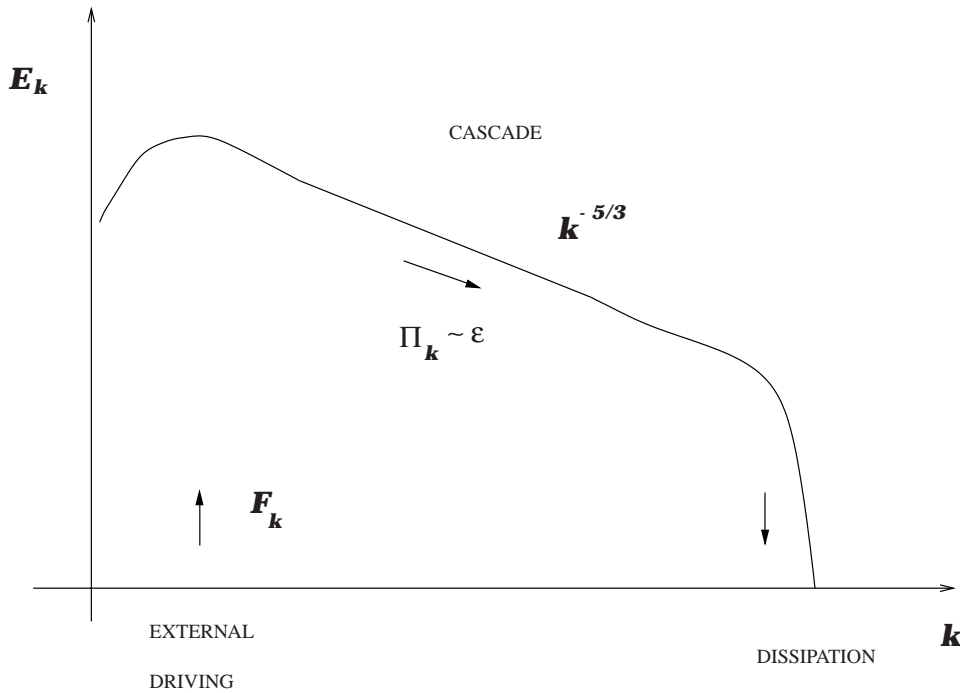


Figure 2. Sketch of the Kolmogorov spectrum for hydrodynamic turbulence.

numerical simulations (Lilly, 1969; Herring and Kraichnan, 1972; Fyfe, Montgomery, and Joyce, 1977; Meneguzzi, Frisch, and Pouquet, 1981; Matthaeus and Lamkin, 1986; Biskamp and Welter, 1989; Politano, Pouquet, and Sulem, 1989).

MHD turbulence displays two rather different regimes, depending on the value of the plasma parameter β , which is the ratio between gas pressure and magnetic pressure. For values of β much larger than unity, the dynamics is dominated by the velocity field. Therefore, the turbulence is essentially hydrodynamic, and corresponds to the Kolmogorov scenario outlined above. This regime probably provides a reasonable description of photospheric motions away from sunspots (see Nesis *et al.*, 1999), where the relatively tenuous magnetic field is simply being advected by the velocity field. On the other hand, the very low β plasma confined in coronal loops, follows a magnetically dominated regime. Turbulent fluctuations are perpendicular to the main (macroscopic) magnetic field \mathbf{B}_0 , and consequently small scales develop along planes perpendicular to \mathbf{B}_0 . In this regime, the total energy (i.e., kinetic plus magnetic) follows a direct cascade, and a Kraichnan spectrum is developed in the energy inertial region (for a recent review on MHD turbulence, see for instance Biskamp, 1993). The Kraichnan spectrum, $E_k \simeq k^{-3/2}$, is derived following scaling arguments similar to Kolmogorov's, but including the effect of Alfvén waves traveling along macroscopic magnetic field structures (Kraichnan, 1965). It is important to stress that in this low- β regime, magnetic field lines are not

simply being advected by footpoint motions, but also generate their own non-linear response to the forcing, developing small scale structures, as shown below.

We numerically explore the feasibility of a turbulent scenario for coronal loops, describing the internal dynamics of loops through the RMHD approximation. We assume periodicity for the lateral boundary conditions, and specify the velocity fields at the $z = 0$ and $z = L$ photospheric boundaries. In particular, we assume

$$\psi(z = 0) = 0, \quad \psi(z = L) = \Psi(x, y), \quad (8)$$

where $\Psi(x, y)$ is the stream function which describes stationary and incompressible footpoint motions on the photospheric plane. The strength of this external velocity field is therefore proportional to a typical photospheric velocity V_p ($V_p \approx 1 \text{ km s}^{-1}$).

To transform Equations (5)–(6) into their dimensionless form, we choose l_p and L as the units for transverse and longitudinal distances ($l_p \approx 10^3 \text{ km}$ and $L \approx 10^4 - 10^5 \text{ km}$) and $t_A \equiv L/v_A$ as the time unit ($t_A \approx 10 - 100 \text{ s}$). The dimensionless RMHD equations are:

$$\partial_t a = \partial_z \psi + [\psi, a] + \frac{1}{S} \nabla_{\perp}^2 a, \quad (9)$$

$$\partial_t w = \partial_z j + [\psi, w] - [a, j] + \frac{1}{R} \nabla_{\perp}^2 w, \quad (10)$$

where $S = l_p^2/\eta t_A$ and $R = l_p^2/v t_A$ are respectively the magnetic and kinetic Reynolds numbers. For typical coronal conditions, these numbers lie within the range $R \approx S \approx 10^{10} - 10^{12}$. For simplicity, hereafter we will consider the case $S = R$.

For the numerical simulation of these equations, the magnetic vector potential and the stream function are expanded in Fourier modes in each plane (x, y) , i.e.,

$$a(x, y, z, t) = \sum_{\mathbf{k}} a_{\mathbf{k}}(z, t) e^{i\mathbf{k}\cdot\mathbf{x}}, \quad (11)$$

$$\psi(x, y, z, t) = \sum_{\mathbf{k}} \psi_{\mathbf{k}}(z, t) e^{i\mathbf{k}\cdot\mathbf{x}}. \quad (12)$$

The equations for the coefficients $\psi_{\mathbf{k}}(z, t)$ and $a_{\mathbf{k}}(z, t)$ are time-evolved using a semi-implicit scheme (for details, see Dmitruk and Gómez, 1999). Linear terms are treated in a fully implicit fashion, while nonlinear terms are evolved using a predictor-corrector scheme. Also, nonlinear terms are evaluated following a $\frac{2}{3}$ fully de-aliased (Canuto *et al.*, 1988) pseudo-spectral technique. To compute z -derivatives we use a standard method of finite differences in a staggered regular grid (Strauss, 1976).

We model the photospheric boundary motion in Equation (8) as $\Psi_{\mathbf{k}} = \Psi_0 = \text{constant}$ inside the ring $3 < kl_p < 4$, and $\Psi_{\mathbf{k}} = 0$ elsewhere, to simulate a

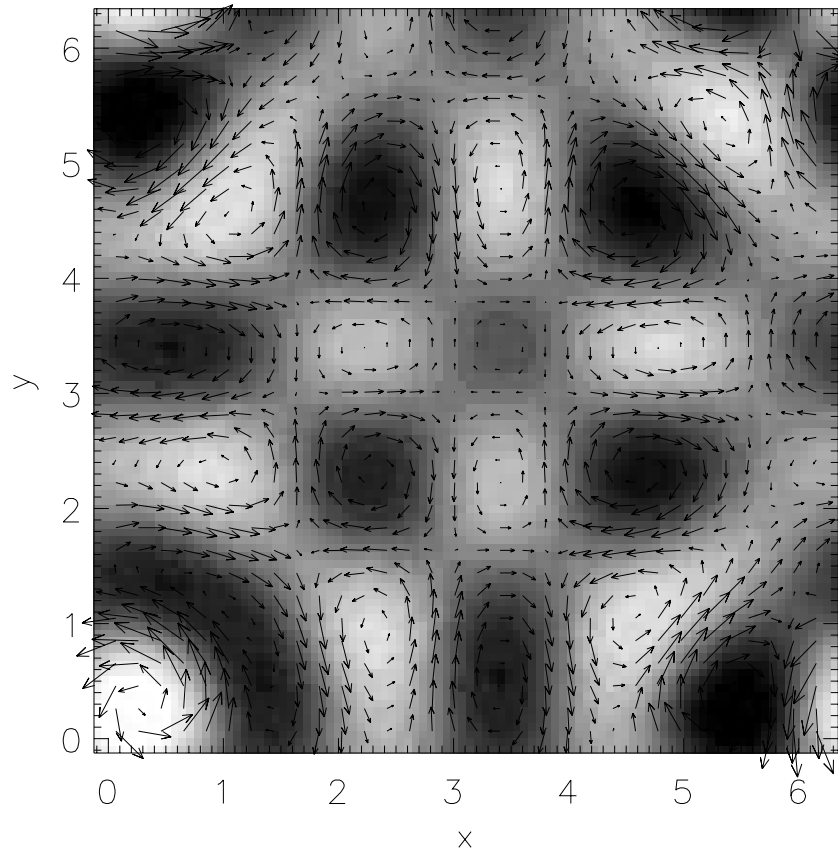


Figure 3. Velocity field applied to the upper boundary ($z = L$). The half-tone shows the stream function and the arrows correspond to the velocity field.

stationary and isotropic pattern of photospheric granular motions of diameters between $2\pi l_p/4$ and $2\pi l_p/3$ (see Figure 3). The typical time-scale associated to these driving motions is the eddy turnover time, which is defined as $t_p = l_p/V_p \approx 10^3$ s. We chose a narrow-band and non-random forcing to make sure that the broadband energy spectra and the signatures of intermittency that we obtained (see below) are exclusively determined by the nonlinear nature of the MHD equations. Resonant interactions between Fourier modes are found to trigger nonlinear instabilities, thus contributing to generate fine spatial structure inside externally driven loops (Gómez, De Luca, and McClymont, 1995). It is important to note that recent observations of solar granulation (see, for instance, Nesis *et al.*, 1999) and references therein), show a very rich dynamical structure, with clear indications of the presence of intermittent hydrodynamic turbulence. However, it seems apparent that if this narrow-band and stationary forcing is able to develop a turbulent regime, more realistic photospheric motions will develop turbulence much easier.

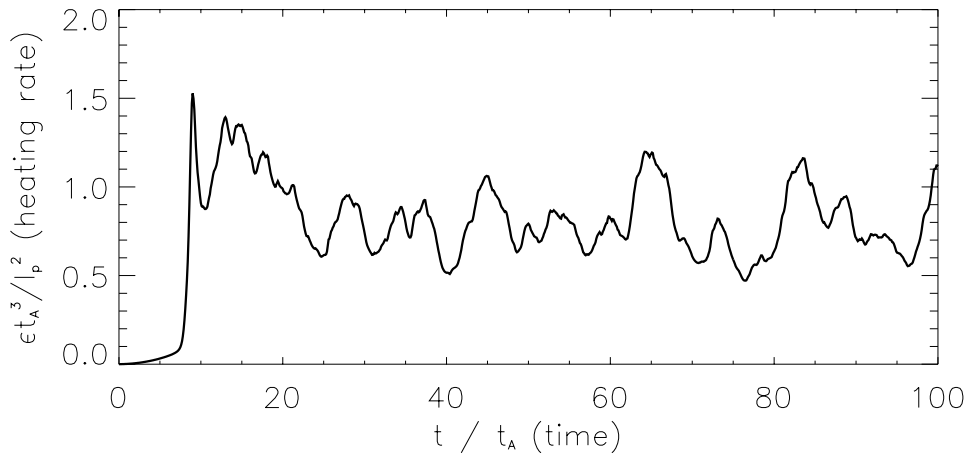


Figure 4. Energy dissipation rate vs time for $t_A/t_p = 0.064$.

We performed a sequence of numerical simulations of Equations (9) and (10) with $192 \times 192 \times 32$ grid points, $S = 1500$ and several values of the ratio t_A/t_p spanning the range $[0.01, 0.15]$ (Dmitruk and Gómez, 1999). The typical behavior of the heating rate ϵ as a function of time, is shown in Figure 4 for the particular case of $t_A/t_p = 0.064$ in dimensionless units. After an initial transient, the heating rate is seen to approach a stationary level.

This level is fully consistent with the heating requirements for coronal active regions of $10^7 \text{ erg cm}^{-2} \text{ s}^{-1}$ (Withbroe and Noyes, 1977). The intermittent behavior of this time series, which is typical of turbulent systems, is also ubiquitous in all our simulations. Once the stationary regime is reached in each of the simulations, we determine the mean value and rms of the departure of the series from the mean.

For both two- and three-dimensional MHD turbulence, the development of a Kraichnan power spectrum is expected, i.e., $E_k \simeq k^{-3/2}$ (Kraichnan, 1965). To compute the energy power spectrum, we performed a single simulation with better spatial resolution ($384 \times 384 \times 32$) and $S = 5000$. The spectrum shown in Figure 5 was taken at $t = 5t_p$, i.e., well in the stationary regime. The obtained slope is consistent with a Kraichnan spectrum. Also, note that the kinetic and magnetic power spectra reach equipartition at large wavenumbers, even though the total kinetic energy is much smaller than the total magnetic energy.

Another important consequence of the energy power spectrum displayed in Figure 5 is the fact that smaller scales dissipate more energy than the larger scales, since $\epsilon_k \sim k^2 E_k \simeq k^{1/2}$. The morphology of small-scale dissipative structures in MHD turbulence has been readily investigated, both in three-dimensional (Mikic, Schnack, and van Hoven, 1989; Longcope and Strauss, 1994; Longcope and Sudan, 1994; Galsgaard and Nordlund, 1996; Milano *et al.*, 1999) and two-dimensional simulations (Matthaeus and Lamkin, 1986; Biskamp and Welter, 1989; Dmitruk, Gómez, and DeLuca, 1998), and have been characterized as elongated current

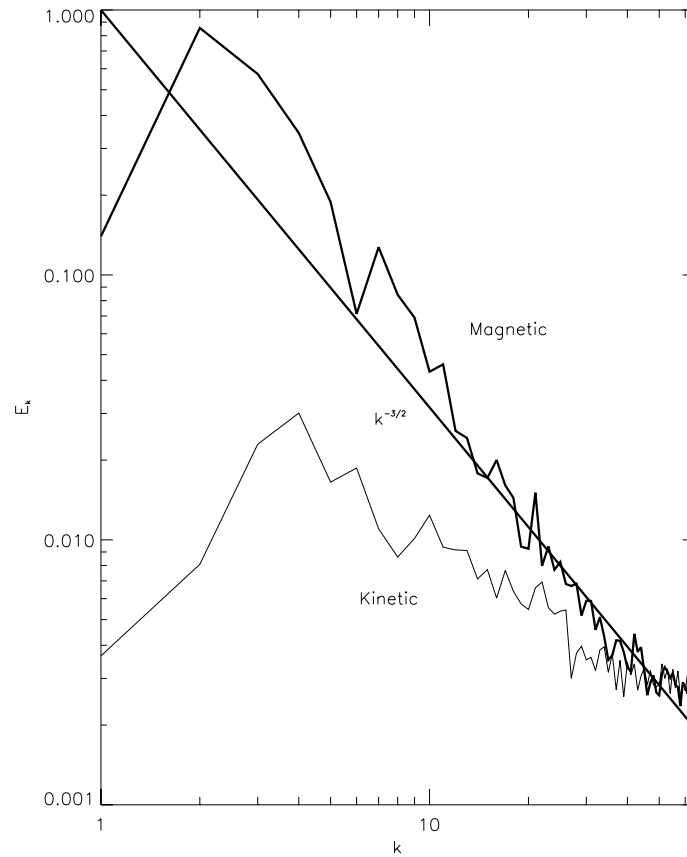


Figure 5. Energy power spectrum for the $384 \times 384 \times 32$ simulation at $t = 5t_p$.

sheets. Figure 6 shows the spatial distribution of the electric current density $j(x, y, z, t)$ for our $384 \times 384 \times 32$ simulation ($t_A/t_p = 0.064$ and $S = 5000$). The presence of elongated current sheets as the most common dissipative structures is also apparent in these simulations.

Figure 7 shows the spatial distribution of current density in a transverse slice at half length of the loop (Figure 7(a)). The arrows correspond to the magnetic field components on that plane. In spite of the artificially small Reynolds number of the simulation, a rich spatial structure can be observed, with current sheets and O-points.

Figure 7(b) also shows the spatial distribution of vorticity for the same slice, and the arrows correspond to the velocity field. The typical quadrupole structures for the vorticity and the alfvénic outflows associated to the current sheets can be observed. Furthermore, these outflows are seen to generate turbulent transients, characterized by Kraichnan energy power spectra (Hendrix and van Hoven, 1996; Milano *et al.*, 1999).



Figure 6. Spatial distribution of currents. The iso-current surface corresponds to $j = 0.3j_{\max}$.

From these simulations, we can also derive a turbulent velocity for coronal loops, which is simply the square root of the total kinetic energy (Dmitruk, Gómez, and DeLuca, 1998). These turbulent velocities range between 10 and 20 km s⁻¹. These values are quite comparable to those derived from line broadening of EUV spectral lines, both with SUMER (Seely *et al.*, 1997; Chae, Schuhle, and Lemaire, 1998) and CDS (Harra-Murnion *et al.*, 1999), which in turn confirm earlier measurements (Cheng, Doschek, and Feldman, 1979). These turbulent velocities, however, are noticeably smaller than those derived from SMM data (Saba and Strong, 1991), which presumably correspond to much hotter and larger active regions.

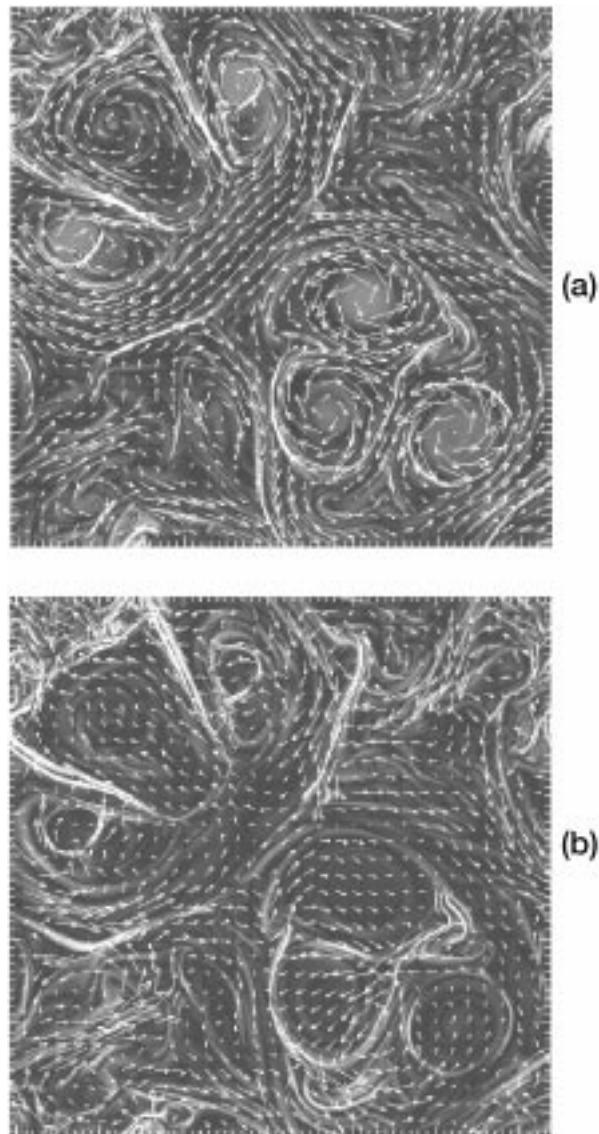


Figure 7. (a) Transverse slice at half length of a loop. The half-tone indicates electric current density flowing across this plane. The arrows correspond to the magnetic field components on this plane. (b) Same transverse slice. The half-tone indicates the vorticity component perpendicular to this plane. The arrows correspond to the velocity field.

5. Scaling Law

As mentioned in the previous section, the Reynolds number ($S = R$) is the only dimensionless parameter explicitly present in Equations (9) and (10). The boundary condition (Equation (8)) brings a second dimensionless parameter into play, namely the ratio between the photospheric velocity V_p and our velocity unit l_p/t_A . Since $V_p = l_p/t_p$, this velocity ratio is equivalent to the ratio between the Alfvén time t_A and the photospheric turnover time t_p .

It is essential to note at this point that to integrate Equations (9) and (10) with the boundary condition Equation (8), only two dimensionless parameters are needed: S and t_A/t_p . Therefore, from purely dimensional considerations, we can derive the following important result: *for any physical quantity, its dimensionless version Q should be an arbitrary function of the only two dimensionless parameters of the problem, i.e.,*

$$Q = \mathcal{F} \left(\frac{t_A}{t_p}, S \right). \quad (13)$$

For the important case of the heating rate per unit mass, i.e., ϵ/ρ , its dimensionless version is

$$Q = \frac{\epsilon t_A^3}{\rho l_p^2} = \mathcal{F} \left(\frac{t_A}{t_p}, S \right). \quad (14)$$

One of Kolmogorov's hypotheses in his celebrated theory for stationary turbulent regimes at very large Reynolds numbers (Kolmogorov, 1941) states that the dissipation rate is independent of the Reynolds number (see also Frisch, 1996). We have already shown that externally driven coronal loops eventually reach a stationary turbulent regime. If we therefore assume that the dissipation rate ϵ is largely independent of the Reynolds number S , we obtain

$$\epsilon = \frac{\rho l_p^2}{t_A^3} \mathcal{F} \left(\frac{t_A}{t_p} \right). \quad (15)$$

From a sequence of numerical simulations for different values of the ratio t_A/t_p (Dmitruk and Gómez, 1999), we find that the function \mathcal{F} is a power law with a slope $s = 1.51 \pm 0.04$, i.e.,

$$\epsilon \propto \frac{\rho l_p^2}{t_A^3} \left(\frac{t_A}{t_p} \right)^{3/2}. \quad (16)$$

This result is fully consistent with the prediction arising from a two-dimensional MHD model (Dmitruk and Gómez, 1997), $s_{2D} = \frac{3}{2}$, which is assumed to simulate the dynamics of a generic transverse slice of a loop. This coincidence between both scalings suggests that two-dimensional simulations provide an adequate description of the dynamics of coronal loops (Hendrix and van Hoven, 1996; Matthaeus

et al., 1998; Oughton, Gosh, and Matthaeus, 1998), provided that the external forcing in Equations (5) and (6) is approximated as (Einaudi *et al.*, 1996; Dmitruk and Gómez, 1997)

$$f = v_A \partial_z \psi \approx \frac{l_p V_p}{t_A}, \quad g = v_A \partial_z j \approx 0, \quad (17)$$

which stems from the assumption that field lines remain relatively straight while their footpoints are being moved about. In this two-dimensional version of the problem, parameters such as V_p , v_A and L arise only indirectly, through the forcing term f (see Equation (5)). As in the previous section, we also assume: (i) a typical granule length scale l_p for the forcing and, (ii) a dissipation rate ϵ independent of the Reynolds number S . Therefore, from dimensional arguments we find that the heating rate per unit mass (ϵ/ρ) can only depend on the relevant parameters l_p and f in the following fashion:

$$\frac{\epsilon}{\rho} \sim \frac{f^3}{l_p} = \frac{l_p^2}{t_A^3} \left(\frac{t_A}{l_p} \right)^{3/2}, \quad (18)$$

which exactly matches the scaling derived empirically from the sequence of RMHD simulations (see Equation (16)). Alternative laws have been derived by other authors (Hendrix *et al.*, 1996) considering two extra parameters, namely, a mild dependence on the Reynolds number S and a photospheric correlation time (apart from the granules turnover time).

Scaling laws like the one displayed in Equation (16), corresponding to a wide variety of coronal heating theories, have been reviewed in an excellent paper by Mandrini, Démoulin, and Klimchuk (2000). In their study, the authors report a statistical correlation between the lengths of loops and their average magnetic field, based on magnetogram extrapolations for a large number of active regions. This correlation has the form $\langle B \rangle \sim L^{-0.9 \pm 0.3}$, confirming an earlier result (Porter and Klimchuk, 1995). By combining this law with the approximate dependence of the heating rate like L^{-2} (arising from a static balance between a uniform heating source, thermal conduction and radiative losses), they can test different models of coronal heating. They find that DC models are in generally better agreement with these observational constraints than AC heating models.

6. Statistics of Events

To perform extended time simulations we focus on the dynamics in a given transverse plane, that is, we study the evolution of a generic two-dimensional slice of a loop. To this end, we model the $v_A \partial_z$ terms as indicated in the previous section.

In spite of the narrow forcing and even though velocity and magnetic fields are initially zero, nonlinear terms quickly populate all the modes across the spectrum and a turbulent state develops, with features quite comparable to the ones displayed

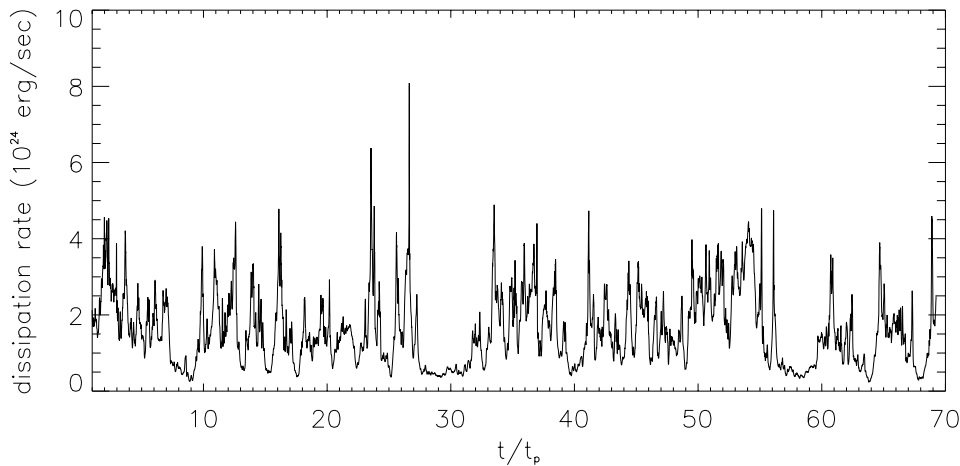


Figure 8. Energy dissipation rate vs time.

by the RMHD equations. Long time-series of the energy dissipation rate are obtained, as the one shown in Figure 8. These time series exhibit the intermittent behavior also shown in Figure 4 for the RMHD case, which is characteristic of turbulent systems.

Parker (1988) proposed that the energy dissipation of the stressed magnetic structures takes place in a large number of small events, which he termed ‘nanoflares’. The superposition of a large number of such events would give the global appearance of a spatially homogeneous and stationary heating process. From a turbulent scenario, it seems straightforward to relate this spiky (both in space and time) heating, to the internal intermittency present in all turbulent regimes. We therefore associate the peaks of energy dissipation displayed in Figure 8 to the so-called nanoflares (Dmitruk and Gómez, 1997; Dmitruk, Gómez, and DeLuca, 1998). We estimate the occurrence rate for these nano-events, i.e., the number of events per unit energy and time, $P(E) = dN/dE$, so that

$$\mathcal{R} = \int_{E_{\min}}^{E_{\max}} dE P(E) \quad (19)$$

is the total number of events per unit time and

$$\epsilon(2\pi l_p)^2 L = \int_{E_{\min}}^{E_{\max}} dE E P(E) \quad (20)$$

is the total heating rate (in erg s^{-1}) contributed by all events in the energy range $[E_{\min}; E_{\max}]$. We define events simply as the excesses of dissipation with respect to a threshold value ϵ_0 of the order of the heating rate time average. Further details

of this derivation can be found elsewhere (Dmitruk and Gómez, 1997; Dmitruk, Gómez, and DeLuca, 1998).

The occurrence rate as a function of energy is found to display a power-law behavior

$$P(E) = AE^{-1.5 \pm 0.2}, \quad (21)$$

in the energy range spanned from $E_{\min} \simeq 10^{25}$ erg to $E_{\max} \simeq 2 \times 10^{26}$ erg. We also computed the distribution of events as a function of peak fluxes which is a power law with slope $\alpha_P = 1.7 \pm 0.3$ (Dmitruk, Gómez, and DeLuca, 1998). This slope is consistent with the one derived by Crosby, Aschwanden, and Dennis (1993) (1.68) from X-ray events and somewhat flatter than those reported by Hudson (1991) (1.8). Similar event distributions have been derived by other authors, both from MHD simulations (Georgoulis, Velli, and Einaudi, 1998) and from cellular automata models (Lu and Hamilton, 1991; Lu *et al.*, 1993; Vlahos *et al.*, 1995). Other important results from this statistical analysis are the correlations between the different parameters of these events. For instance, the energy released vs event duration τ can be fitted by a power law $E \sim \tau^2$ (Dmitruk, Gómez, and DeLuca, 1998). This result is consistent with the correlation reported by (Lee, Petrosian, and McTiernan, 1993) from hard X-ray observations.

7. Conclusion

The main results of the present study can be summarized as follows:

(1) TRACE movies show that coronal active regions are extremely dynamic and inhomogeneous objects. This ubiquitous spatial and temporal variability suggests the presence of a rather intermittent heating mechanism for these regions. We propose that the development of MHD turbulence in coronal loops driven at their footpoints will naturally produce intermittent dissipation.

(2) Numerical integrations of the RMHD equations, driven by a stationary pattern of large-scale footpoint motions show that the system reaches a turbulent stationary regime, characterized by a Kraichnan energy power spectrum. Also, the ensuing energy cascade enhances the average dissipation rate to the levels required by the conductive and radiative losses of the coronal plasma. Most of the dissipation occurs in current sheets approximately parallel to the loop axis.

(3) The MHD turbulence developed in coronal loops is magnetically dominated, i.e., the magnetic energy is much larger than the kinetic energy. Turbulent velocities of about 10–20 km s⁻¹ are obtained, which are fully consistent with those inferred by various authors from the broadening of EUV spectral lines.

(4) By combining dimensional arguments on the RMHD equations with a sequence of numerical simulations, a scaling law is derived, which relates the turbulent heating rate with the various relevant physical parameters (Dmitruk and Gómez, 1999). This kind of scaling law, arising from theoretical heating models,

can be tested against observational constraints (Mandrini, Démoulin, and Klimchuk, 2000).

(5) The intermittent nature of energy dissipation suggests that the heating mechanism can be interpreted as a stochastic superposition of discrete events or *nanoflares* (Parker, 1988). In this regard, it is important to note that the turbulent scenario is not inconsistent with Parker's scenario (Longcope and Sudan, 1994; Hendrix *et al.*, 1996). Furthermore, it could perhaps be considered as its natural extension to dissipative plasmas, since the tangential discontinuities arising in an ideal plasma will become thin current sheets if a small amount of dissipation is allowed. A statistics of dissipation events obtained from numerical simulations, yields a power law energy occurrence rate. The slope of this distribution is approximately 1.5, which is quite comparable to similar analysis performed for the occurrence of flares (Hudson, 1991; Crosby, Aschwanden, and Dennis, 1993) and microflares (Shimizu, 1995).

Acknowledgements

The authors wish to express their gratitude to the local organizers of the Physics of the Solar Corona and Transition Region Workshop, where this paper was presented, Drs Karel Schrijver, Zoe Frank, and Neal Hurlburt, for such a superb meeting and for their kind hospitality. This work is supported by the University of Buenos Aires (grant UBACYT TX065/98), and the Agencia Nacional de Promoción de Ciencia y Tecnología (grant PICT 02305/97). DG is Member of the Carrera del Investigador Científico of CONICET, Argentina.

References

- Biskamp, D.: 1993, *Nonlinear Magnetohydrodynamics*, Cambridge University Press, Cambridge.
- Biskamp, D. and Welter, H.: 1989, *Phys. Fluids* **B1**, 1964.
- Canuto, C., Hussaini, M. Y., Quarteroni, A., and Zang, T. A.: 1988, *Spectral Methods in Fluid Dynamics*, Springer-Verlag, New York.
- Chae, J., Schuhle, U., and Lemaire, P.: 1998, *Astrophys. J.* **505**, 957.
- Cheng, C., Doschek, G. and Feldman U.: 1979, *Astrophys. J.* **227**, 1037.
- Crosby, N. B., Aschwanden, M. J., and Dennis, B. R.: 1993, *Solar Phys.* **143**, 275.
- Dmitruk, P. and Gómez, D. O.: 1997, *Astrophys. J.* **484**, L83.
- Dmitruk, P. and Gómez, D.O.: 1999, *Astrophys. J.* **527**, L63.
- Dmitruk, P., Gómez, D. O., and DeLuca, E. E.: 1998, *Astrophys. J.* **505**, 974.
- Einaudi, G., Velli, M., Politano, H., and Pouquet, A.: 1996, *Astrophys. J.* **457**, L113.
- Frisch, U.: 1996, *Turbulence*, Cambridge University Press, Cambridge.
- Fyfe, D., Montgomery, D., and Joyce, G.: 1977, *J. Plasma Phys.* **17**, 369.
- Galsgaard, K. and Nordlund, A.: 1996, *J. Geophys. Res.* **101**, 13445.
- Georgoulis, M., Velli, M., and Einaudi, G.: 1998, *Astrophys. J.* **497**, 957.
- Golub, L. and Pasachoff, J.: 1997, *The Solar Corona*, Cambridge University Press, Cambridge.

- Golub, L., Herant, M., Kalata, K., Louvas, I., Nystrom, G., Pardo, F., Spiller, E., and Wilczynski, J. S.: 1990, *Nature* **344**, 842.
- Gómez, D. O.: 1990, *Fund. Cosmic Phys.* **14**, 361.
- Gómez, D. O. and Ferro Fontán, C.: 1988, *Solar Phys.* **116**, 33.
- Gómez, D. O. and Ferro Fontán, C.: 1992, *Astrophys. J.* **394**, 662.
- Gómez, D. O., De Luca, E. E., and Mc Clymont, A. N.: 1995, *Astrophys. J.* **448**, 954.
- Grant, H. L., Stewart, R. W., and Molliet, A.: 1962, *J. Fluid Mech.* **12**, 241.
- Harra-Murnion, L. K., Matthews, S. A., Hara, H., and Ichimoto, K.: 1999, *Astron. Astrophys.* **345**, 1011.
- Hendrix, D. L. and van Hoven, G.: 1996, *Astrophys. J.* **467**, 887.
- Hendrix, D. L., van Hoven, G., Mikic, Z., and Schnack, D. D.: 1996, *Astrophys. J.* **470**, 1192.
- Herring, J. and Kraichnan, R. H.: 1972, in M. Rosenblatt and C. van Atta (eds.), 'Statistical Models and Turbulence', Springer-Verlag, Berlin.
- Heyvaerts, J. and Priest, E. R.: 1983, *Astron. Astrophys.* **117**, 220.
- Heyvaerts, J. and Priest, E. R.: 1992, *Astrophys. J.* **390**, 297.
- Hollweg, J. V.: 1985, in B. Buti (ed.), *Advance Space Plasma Physics*, World Science Publ. Co., Singapore, p. 77.
- Hudson, H. S.: 1991, *Solar Phys.* **133**, 357.
- Ionson, J. A.: 1982, *Astrophys. J.* **254**, 318.
- Kolmogorov, A. N.: 1941, *Dokl. Acad. Sci. URSS* **30**, 301.
- Kraichnan, R. H.: 1965, *Phys. Fluids* **8**, 138.
- Lee, T. T., Petrosian, V., and McTiernan, J. M.: 1993, *Astrophys. J.* **412**, 401.
- Lilly, D. K.: 1969, *Phys. Fluids* **12**, 240.
- Longcope, D. W. and Strauss, H. R.: 1994, *Astrophys. J.* **426**, 742.
- Longcope, D. W. and Sudan, R. N.: 1994, *Astrophys. J.* **437**, 491.
- Lu, E. T. and Hamilton, R. J.: 1991, *Astrophys. J.* **380**, L89.
- Lu, E., Hamilton, R., McTiernan, J., and Bromund, K.: 1993, *Astrophys. J.* **412**, 841.
- Mandrini, C. H., Démoulin, P., and Klimchuk, J. A.: 2000, *Astrophys. J.* **530**, in press.
- Matthaeus, W. H., and Goldstein, G. L.: 1982, *J. Geophys. Res.* **87**, 6011.
- Matthaeus, W. H. and Lamkin, S. L.: 1986, *Phys. Fluids* **29**, 2513.
- Matthaeus, W. H., Oughton, S., Ghosh, S., and Hossain, M.: 1998, *Phys. Rev. Letters* **81**, 2056.
- Meneguzzi, M., Frisch, U., and Pouquet, A.: 1981, *Phys. Rev. Letters* **47**, 1060.
- Mikic, Z., Schnack, D. D., and van Hoven, G.: 1989, *Astrophys. J.* **338**, 1148.
- Milano, L. J., Gómez, D. O., and Martens, P. C. H.: 1997, *Astrophys. J.* **490**, 442.
- Milano, L. J., Dmitruk, P., Mandrini, C. H., Gómez, D. O., and Démoulin, P.: 1999, *Astrophys. J.* **521**, 889.
- Montgomery, D.: 1983, in M. Neugebauer (ed.), 'Solar Wind V', NASA Conf. Publ. 2280, p. 107.
- Nakariakov, V. M., Ofman, L., DeLuca, E. E., Roberts, B., and Davila, J. M.: 1999, *Nature* **285**, 862.
- Narain, U. and Ulmschneider, P.: 1990, *Space Sci. Rev.* **54**, 377.
- Narain, U. and Ulmschneider, P.: 1996, *Space Sci. Rev.* **75**, 453.
- Nesis, A., Hammer, R., Kiefer, M., Schleicher, H., Sigwarth, M., and Staiger, J.: 1999, *Astron. Astrophys.* **345**, 265.
- Ofman, L., Davila, J. M., and Steinolfson, R. S.: 1995, *Astrophys. J.* **444**, 471.
- Oughton, S., Ghosh, S., and Matthaeus, W. H.: 1998, *Phys. Plasmas* **5**, 4235.
- Parker, E. N.: 1972, *Astrophys. J.* **174**, 499.
- Parker, E. N.: 1983, *Astrophys. J.* **264**, 642.
- Parker, E. N.: 1988, *Astrophys. J.* **330**, 474.
- Politano, H., Pouquet, A., and Sulem, P. L.: 1989, *Phys. Fluids* **B1**, 2330.
- Porter, L. J. and Klimchuk, J. A.: 1995, *Astrophys. J.* **454**, 499.
- Saba, J. and Strong, K.: 1991, *Astrophys. J.* **375**, 789.
- Schrijver, C. J. and 16 co-authors: 1999, *Solar Phys.*, **187**, 261.

- Seely, N. *et al.*: 1997, *Astrophys. J.* **484**, L87.
Shimizu, T.: 1995, *Publ. Astr. Soc. Japan* **47**, 251.
Sommeria, J.: 1986, *J. Fluid Mech.* **170**, 139.
Strauss, H.: 1976, *Phys. Fluids* **19**, 134.
van Ballegooijen, A. A.: 1986, *Astrophys. J.* **311**, 1001.
Vlahos, H., Georgoulis, M., Kluiving, R., and Paschos, P.: 1995, *Astron. Astrophys.* **299**, 897.
Withbroe, G. L. and Noyes, R. W.: 1977, *Ann. Rev. Astron. Astrophys.* **15**, 363.
Zirker, J. B. 1993, *Solar Phys.* **148**, 43.